

Zn- and Cd-induced features at the GaAs(110) and InP(110) surfaces studied by low-temperature scanning tunneling microscopy

R. de Kort, M. C. M. M. van der Wielen, A. J. A. van Roij, W. Kets, and H. van Kempen
Research Institute for Materials, University of Nijmegen, Toernooiveld 1, 6525 ED Nijmegen, The Netherlands
 (Received 27 October 1999; revised manuscript received 19 September 2000; published 13 March 2001)

We used a low-temperature scanning tunneling microscope to study Zn- and Cd-doping atoms near the (110)-cleavage surfaces of GaAs and InP at 4.2 K. The filled-state images showed centro-symmetric elevations while the empty-state images showed circular depressions. We attribute these features to the influence of the Coulomb potential of the ionized doping atoms on the number of states available for tunneling. In a few empty-state images of the GaAs(110) surface, the depressions were surrounded by maxima, which are probably direct observations of Friedel oscillations. For the InP(110) surface, all depressions were surrounded by noncentrosymmetric maxima. Upon moving the tip Fermi level to the bottom of the conduction band, we observed that the depressions turned into elevations with a triangular shape for both the GaAs(110) and the InP(110) surface. This shape was independent of the depth of the dopants, and the chemical nature of the dopants (Zn or Cd) did not influence the triangular shape either. The orientation of these triangular features was the same for all observed doping atoms and was geometrically determined with respect to the host lattice. Furthermore, we determined the location of a triangular feature with respect to a doping atom. The features were only visible when tunneling to the impurity band suggesting that the features are a direct image of the acceptor state although the origin of the triangular shape is not clear at present.

DOI: 10.1103/PhysRevB.63.125336

PACS number(s): 68.37.Ef, 68.35.Dv, 71.55.Eq, 73.20.Hb

I. INTRODUCTION

Doped semiconductors are commonly used in industry, yet the behavior of doping atoms is still not fully understood. Since electronic devices are getting smaller and smaller, their characteristics will be influenced by fewer and, eventually, even single-lattice imperfections, e.g., doping atoms, antisite defects, and vacancies. These imperfections can be studied individually on an atomic scale with a scanning tunneling microscope (STM).

Many STM studies have been carried out on III-V semiconductors. The (110)-cleavage surfaces of these semiconductors are ideal for studying bulk imperfections with a surface-sensitive tool such as an STM, because there are no surface states inside the bulk energy band gap of III-V semiconductor surfaces. Therefore, bulk effects are not screened at the surface. Reference 1 gives an overview of STM observations of charged doping atoms and charged defects on (110)-cleavage surfaces of III-V semiconductors.

Doping atoms are usually imaged as spherical protrusions or depressions in the surface topography depending on sample voltage and their charge.¹⁻⁴ These protrusions or depressions are a direct consequence of the influence of the charge and the corresponding Coulomb potential of the dopants on the number of states available for tunneling. The doping atom depth at which its influence can still be seen at the surface varies from approximately five subsurface layers at room temperature to approximately 15 subsurface layers at 4.2 K.⁵ Oscillations in the charge density (so-called Friedel oscillations) surrounding charged dopants have been observed at 4.2 K,^{6,7} which was attributed to screening of charged dopants by free charge carriers. At room temperature, no Friedel oscillations have been observed, probably

because the amplitude of the dopant-induced features decays faster than at 4.2 K. Nevertheless, recent room-temperature STM measurements showed dark depression rings surrounding bright elevations in STM images of charged dopants and defects.¹ However, these rings were not attributed to an oscillating potential (e.g., charge-density waves, Friedel oscillations), but they were explained as the image of a local potential change (a screened Coulomb potential was used) induced by the presence of the charge.

In this paper, we describe a low-temperature STM study of Zn- and Cd-doping atoms near the (110)-cleavage surfaces of GaAs and InP at 4.2 K. We observed spherical protrusions and depressions in the surface topography for negative and positive sample voltages, respectively, and we attribute them to the Zn- and Cd-doping atoms; however, for small positive sample voltages we observed a different behavior of the dopants: upon moving the tip Fermi level to the bottom of the conduction band, we observed that the depressions turned into elevations with a triangular shape for both the GaAs(110) and the InP(110) surface. A similar triangular shape has previously been observed on the (110)-cleavage surface of *p*-type GaAs (doped with Zn) at room temperature by Zheng *et al.*,⁸ but a satisfactory explanation for these triangular features has not been given so far. Furthermore, Zheng *et al.* did not observe any depressions in their empty-state images at higher sample voltages as in our case.

The triangular shape was not influenced by the depth of the doping atoms. We determined the orientation of these triangular features and we found the same orientation for all observed doping atoms. Furthermore, we determined the orientation of a triangular feature with respect to the host lattice. The base of the triangle is positioned along the $[1\bar{1}0]$ direction, and the mirror plane of the feature is parallel to the $[001]$ direction and has the $[1\bar{1}0]$ direction as its normal.

The doping atom is not positioned in the center of the triangle, but more towards the top vertex.

The Cd- and Zn-acceptor atoms in GaAs and the Zn-acceptor atoms in InP gave similar results. Asymmetric features have also been observed on antisite defects,^{9–11} but in contrast to our observations the shape of those features strongly depended on the depth of the dopants. Since the triangular features were only visible when tunneling to the impurity band, we conclude that the features are a direct image of the acceptor state although the origin of the triangular shape is not clear at present.

II. EXPERIMENT

All the experiments were performed in a low-temperature STM at a temperature of 4.2 K. The STM is described in detail in Ref. 12. We equipped the STM with an *in situ* cleaver, which can be controlled from outside the cryostat, in order to cleave our samples *in situ* at 4.2 K. Since the STM is cooled down more than 85°C below the boiling point of oxygen, the vapor pressure of oxygen is extremely low ($<10^{-15}$ Torr). Therefore, surfaces like GaAs(110) and InP(110), which normally oxidize very quickly, will stay clean under these conditions for many days.

We used three different samples: *p*-type Zn-doped GaAs with doping concentration $8 \times 10^{18} \text{ cm}^{-3}$, *p*-type Cd-doped GaAs with doping concentration $7.4 \times 10^{17} \text{ cm}^{-3}$, and *p*-type Zn-doped InP with doping concentration $2.7 \times 10^{18} \text{ cm}^{-3}$.¹³ This gives for the radius of the average volume per dopant: 3.1 nm for the Zn-doped GaAs, 6.9 nm for the Cd-doped GaAs, and 4.5 nm for the Zn-doped InP. If this radius is smaller than the Bohr radius, wave functions of doping atoms overlap, and the localized doping levels are broadened to doping or impurity bands, meaning the sample is degenerate. The Bohr radius for *p*-type GaAs is 1.8 nm and for *p*-type InP 1.3 nm. This means that, in all three cases, we do not have fully degenerate samples.

These samples were cleaved along the (110) planes *in situ* at 4.2 K. All the measurements were done with PtIr tips, cut with scissors, and all the STM images shown in this paper are constant current images. Different tips were used, and we did not observe any differences in the STM images, except for some indications of a change in the work function of the tip of the order of 0.1 eV.

III. RESULTS

Figure 1 shows three STM images together with four plots showing line profiles in the $[1\bar{1}0]$ and $[001]$ direction. The measurements were performed on the Zn-doped GaAs sample. Figure 1(a) is a filled-state image measured at -1.8 V sample voltage. Figures 1(b) and 1(c) are empty-state images measured at $+1.8$ V and $+1.55$ V, respectively. The scan area is $5.4 \times 5.4 \text{ nm}^2$. The observed features are induced by the same Zn-doping atom. The filled-state image shows a hillock feature superimposed on the As sublattice. In the empty-state image in Fig. 1(b), a local depression is visible; however, at lower sample voltage the empty-state image shows a triangular elevation [Fig. 1(c)].

One side of the triangle (the base), shown by the solid line in Fig. 1(c), is positioned along the $[1\bar{1}0]$ direction. The mirror plane of the feature (parallel to the $[001]$ direction) has the $[1\bar{1}0]$ direction as its normal. A line profile through this plane is also plotted in Fig. 1(c) and given by the dashed line along the $[001]$ direction. By making large scan images, we can see whether all the triangular features are oriented in the same direction. For example, Fig. 2 shows two large STM images measured on a Zn-doped and Cd-doped GaAs sample, respectively. Many triangular features are visible, and all features have the same orientation as mentioned above, which is in agreement with the observations in Fig. 1(c). Furthermore, the shape of the triangular features is the same for all observed features, only their intensity varies.

The orientation of the triangular features can be determined by studying the line profiles plotted in Figs. 1(d)–1(g). By examining line profiles 2 and 5 in Fig. 1, the position of the Zn doping atom with respect to the As lattice is determined.¹⁴ Line profile 2 shows only one maximum, which means, using symmetry arguments, that the doping atom is positioned in one of the odd subsurface layers (first, third, fifth, etc.). From line profile 5, one can see that the As atoms around the maximum are lifted asymmetrically: the lower As atom seems to be lifted more strongly than the upper one. This means that the As atoms in the $[00\bar{1}]$ direction are always a little bit closer to the Zn atom than the As atoms on the other side of the maximum. With this observation, the orientation of the triangle is determined completely and given in Fig. 3. Together with the other line profiles in Fig. 1, the location of the triangular feature with respect to the Zn atom can be determined as shown in Fig. 3. One can see that the Zn atom is not positioned in the center of the triangle, but more towards the top vertex.

Figure 4 shows a filled-state image of the Zn-doped InP sample, measured at a sample voltage of -0.80 V. The scan area is $30 \times 30 \text{ nm}^2$. The hillock features superimposed on the P sublattice are induced by negatively charged Zn dopants. Figure 5 shows four STM images of the same surface area of the Zn-doped InP sample at different positive sample voltages. The scan area is $30 \times 30 \text{ nm}^2$. Upon lowering the positive sample voltage from $+2.2$ V to $+1.6$ V, we observed that the Zn-induced features changed from circular depressions into triangular elevations. This behavior is similar to that observed for *p* GaAs. In that case, the depressions changed into elevations at a slightly lower sample voltage (≈ 1.6 V instead of ≈ 1.8 V). Again, the shape of the triangular features is the same for all observed features, only their intensity varies. Furthermore, the depressions are surrounded by noncentrosymmetric maxima, which we did not observe for the *p*-type GaAs samples.

IV. DISCUSSION

The hillock features in Figs. 1(a) and 4 are induced by negatively charged Zn doping atoms (substitutional on gallium or indium sites), which locally increase the number of valence-band states available for tunneling, see for example Ref. 8. To understand the origin of the local depressions in

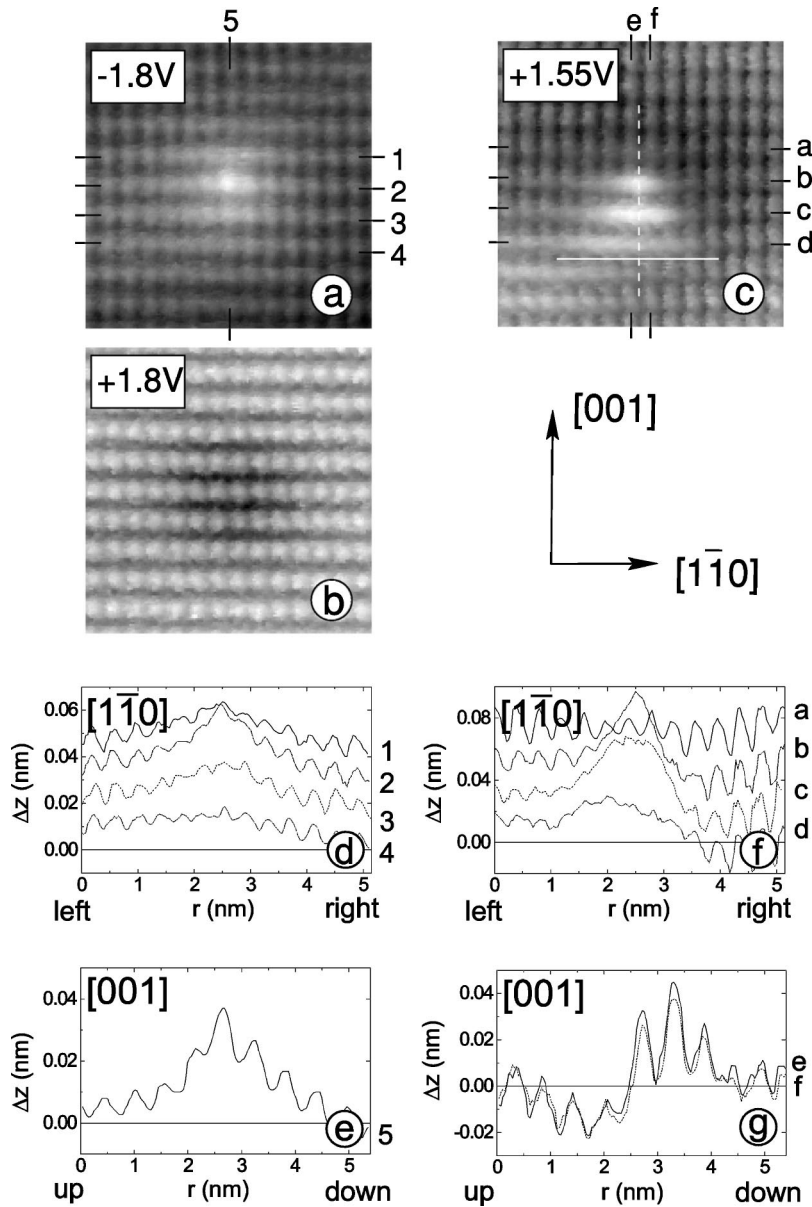


FIG. 1. Three STM images of the same scan area ($5.4 \times 5.4 \text{ nm}^2$) of a Zn-doped GaAs(110) surface (doping concentration: $8 \times 10^{18} \text{ cm}^{-3}$) measured at different sample voltages: (a) -1.8 V , (b) $+1.8 \text{ V}$, (c) $+1.55 \text{ V}$. Set-point current: 100 pA . The meaning of the (dashed) line in figure (c) is explained in the text. (d)–(g) Line profiles through (a) and (c) in the $[1\bar{1}0]$ and $[001]$ direction, respectively. The numbers 1–5 and letters a–f indicate the positions of the different line profiles in (a) and (c), respectively.

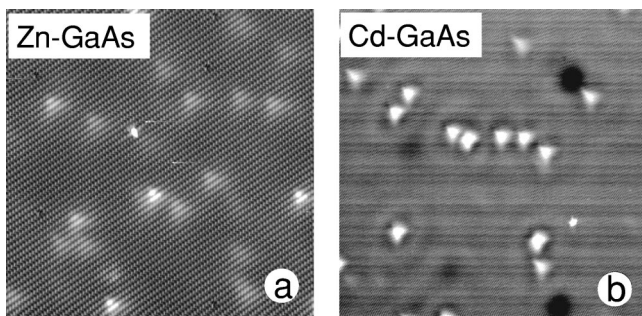


FIG. 2. Two empty-state images of the p -GaAs(110) surface measured on a Zn-doped and Cd-doped sample, respectively. Left: Zn-doping atom. Scan area: $90 \times 90 \text{ nm}^2$. Sample voltage is $+1.8 \text{ V}$, and set-point current is 200 pA . Right: Cd doping atom. Scan area: $100 \times 100 \text{ nm}^2$. Sample voltage is $+1.55 \text{ V}$, and set-point current is 150 pA .

Figs. 1(b) and 5(a), tip-induced band bending at the semiconductor surface has to be taken into account.^{3,4,7,8} The negatively charged Zn atom locally increases the number of valence-band states available for tunneling. As a consequence, the number of conduction-band states available for tunneling is decreased in the vicinity of the Zn impurity. Two tunneling contributions can be distinguished: electrons tunneling from the tip to the empty conduction-band states, and holes coming from the impurity-induced band tunneling to the tip. These contributions are not equal in magnitude: the electrons have to tunnel across a potential barrier that is about 1.5 eV lower (value for the band gaps of GaAs and InP) than the tunnel barrier for holes. The transmission probability for the electrons, which is approximately proportional to $\exp(-2\kappa z)$ with $\kappa = [(2m/\hbar^2)\phi]^{1/2}$ and ϕ the average barrier height, is therefore much higher than it is for holes. For this reason, the contribution from electrons tunneling to the conduction band dominates the tunnel current, and, in particular, conduction-band states are imaged by the STM at

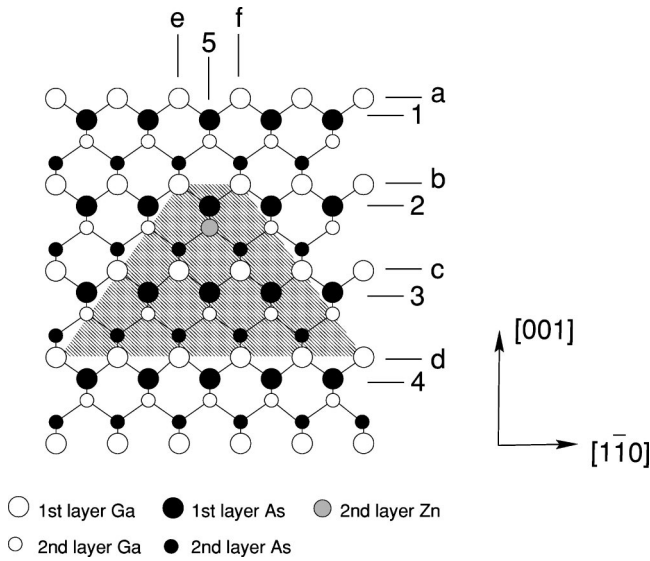


FIG. 3. Schematic representation of the GaAs(110) surface. The first- and second-layer Ga (open circles) and As (closed circles) are plotted. In this figure, the results are summarized that follow from the line profiles in Figs. 1(d)–1(g). The numbers and letters at the top and on the right of the figure correspond to the numbers and letters of the line profiles in Fig. 1. The shaded area roughly describes the region in which the Ga atoms are lifted. The Zn-doping atom is positioned in the second layer, not in the center of the triangle, but more towards the top vertex.

high enough positive sample voltage. Since the number of conduction-band states available for tunneling is reduced in the vicinity of the Zn impurity, a depression in the surface topography is visible as observed in Figs. 1(b) and 5(a).

The contribution from holes coming from the impurity band and tunneling to the metal tip can be increased by decreasing the applied voltage between tip and sample, thus moving towards the band-gap energy of the GaAs or InP sample. Due to the increased number of valence-band states available for tunneling in the vicinity of the Zn dopant, an elevation will be visible in the surface topography. In Figs. 1(c) and 5(d), the depression has indeed been replaced by an elevation in the surface topography. However, the elevation is not circular but has a triangular shape. This has previously been observed on the (110)-cleavage surface of Zn-doped GaAs at room temperature by Zheng *et al.*,⁸ but they did not observe any depressions in their empty-state images at higher sample voltages.

The shape of the triangular features is the same for all observed features, only their intensity varies. Features with smaller intensity are induced by doping atoms located further away from the surface.⁵ From this, we can conclude that the depth of the doping atoms does not influence the shape of the triangular features. The chemical nature of the acceptor atoms probably does not influence the induced features either since both images on the Zn-doped and Cd-doped GaAs samples show comparable results.

As in Ref. 6, Friedel oscillations are to be expected when free charge carriers are accumulated at the surface. For *p*-type GaAs, this is the case for positive sample voltages, in which case holes are accumulated near the surface due to

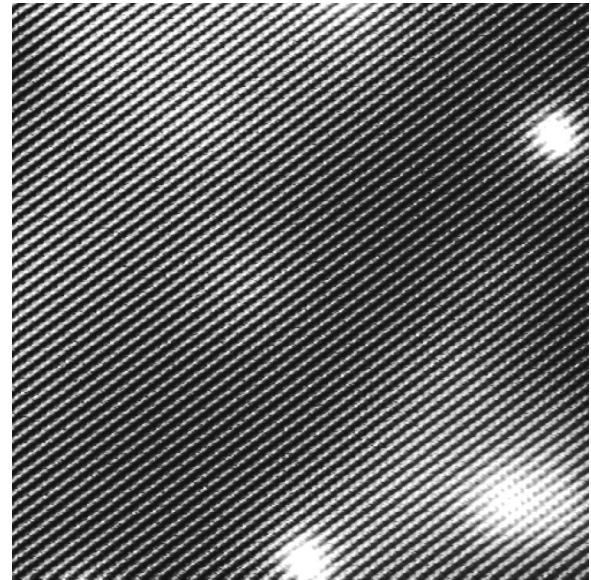


FIG. 4. Filled-state image of the Zn-doped InP(110) surface. Sample voltage: -0.80 V. Set-point current: 100 pA. Scan area: 30×30 nm². Three Zn-induced features can clearly be seen.

tip-induced band bending. However, Friedel oscillations were very difficult to observe in *p*-type GaAs because the corrugation amplitude of the Friedel oscillations was of the same order of magnitude as the corrugation amplitude of the atomic lattice.⁷ In only a few cases did we observe very weak Friedel oscillations in *p*-type GaAs, and an example of these weak oscillations is shown in Fig. 6.

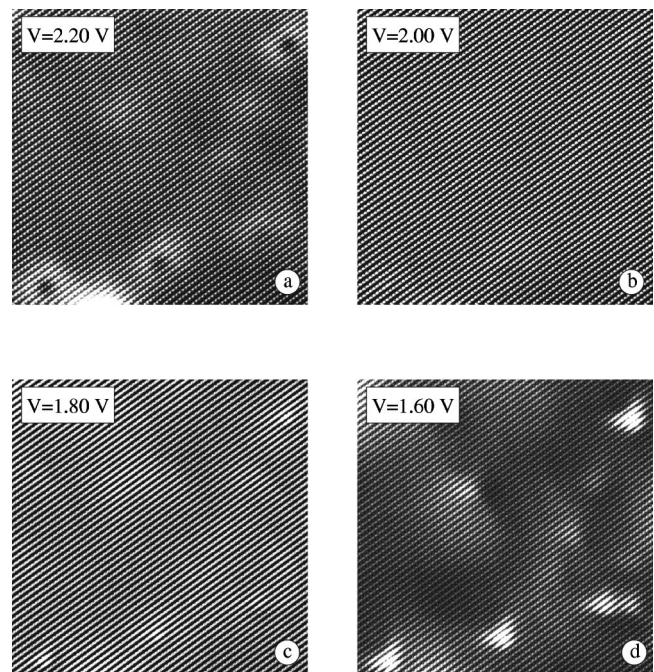


FIG. 5. Four empty-state images of the Zn-doped InP(110) surface. Set-point current: 100 pA. Scan area: 30×30 nm². Sample voltages: (a) $+2.20$ V, (b) $+2.00$ V, (c) $+1.80$ V, (d) $+1.60$ V. If the sample voltage is lowered, the Zn-induced features change from circular depressions into triangular elevations.

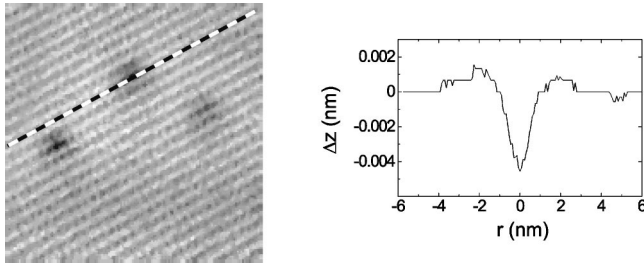


FIG. 6. Left: empty-state image of the Zn-doped GaAs(110) surface. Sample voltage: +2.5 V. Set-point current: 50 pA. Scan area: 11×11 nm². Three Zn-induced features are visible. The circular depressions are surrounded by a maximum. Right: line profile through one of the Zn-induced features indicated by the line. The atomic lattice has been filtered out.

For *p*-type InP, the depressions were surrounded by noncentro-symmetric maxima [Fig. 5(a)], which we did not observe for the *p*-type GaAs samples. The maxima were rather clear, yet no depressions around these maxima could be observed. It is possible that due to the strong decay of the Friedel oscillations only one maximum can be observed, but because of the higher effective mass of holes in InP ($m_h = 0.49m_0$, with m_0 the free-electron mass) than in GaAs ($m_h = 0.37m_0$), Friedel oscillations are expected to be even weaker in *p*-type InP than in *p*-type GaAs.⁷ Since Friedel oscillations were observed only in a few cases in *p*-type GaAs, and since they were already very weak, we do not expect to observe any Friedel oscillations in *p*-type InP. This may indicate that there is only one maximum around each dopant-induced feature, similar to that observed in Ref. 1 although dark rings around bright elevations were found there. These dark rings were explained as the image of a local potential change induced by the presence of the charged dopant. In addition, the asymmetric shape of the maxima has never been observed before. The observed asymmetry could be related to the triangular elevations observed at lower sample voltages. However, the origin of the asymmetry in the maxima observed in our STM images is not clear at present.

The origin of the triangular features is not clear either. We observed these features for *p*-type GaAs doped with Zn and Cd, and for *p*-type InP. Since the feature varies with changing sample voltage, it has to be of an electronic nature. Zheng *et al.*⁸ also reported the observation of triangular features in Zn-doped GaAs at room temperature. However, they observed these triangular features for sample voltages between +1 V and +3 V and did not report any depressions. They discussed possible modification of the electronic state of the Zn dopant due to mechanical distortion of the lattice, which is caused by the difference in atomic radii of Zn and Ga. The radius of a Zn ion is indeed larger than for a Ga ion (0.83 Å and 0.62 Å, respectively), and a Cd ion also has a larger radius (1.03 Å). However, the radius of an In ion is 0.92 Å, which is slightly larger than that for a Zn ion. On the other hand, the Zn dopant is negatively charged, which means that its ionic radius is probably slightly larger, be-

cause the radius of a negative ion is usually larger than its positive counterpart.

Second, we want to compare our observations to those of Feenstra *et al.*⁹ They published observations of noncentrosymmetric features with two satellite structures at the (110) surface of a low-temperature-grown GaAs sample. They proved that the features are induced by isolated subsurface positioned arsenic antisites (As on a Ga site). These features are only visible by STM when tunneling inside the defect-state band. The features extend over a few atomic distances, and the shape is determined by the electron wave functions of the antisite defect. Reference 10 provides a theoretical calculation for these defects showing an intricate interplay of the defect-wave function with the presence of the surface.

Our results are comparable to the results of Feenstra *et al.* The observed triangular features also extend over a few atomic distances and are only visible when tunneling into the impurity-induced energy band. Therefore, the triangle shape could be an image of the wave functions belonging to the acceptor atom. However, it should be noted that in the case of the arsenic antisite features observed by Feenstra *et al.*, the images strongly depend on the depth of the defect while in our case the triangular features are remarkably independent of depth.

Finally, we want to make a qualitative symmetry consideration. Figure 3 shows that the three As first neighbors of the Zn dopant form a triangle whose orientation is the same as that of the observed triangular features. However, the As atoms are negatively charged and are only seen in filled-state images (negative sample voltages), whereas the triangular features are only seen in empty-state images (positive sample voltages), in which case the positive Ga atoms are imaged. The doping atoms might change the ionic bonds between the Ga and As atoms, which might cause the As atoms to influence the STM images at positive sample voltages resulting in the observed triangular features, but we have no further evidence to support this hypothesis. Therefore, we have to conclude that the precise origin of the triangular features is still unknown.

V. SUMMARY

We presented and discussed the dopant-induced features of Zn- and Cd-doped GaAs, and Zn-doped InP measured with a low-temperature STM at 4.2 K. Very weak Friedel oscillations were observed in a few empty-state images of the Zn-doped GaAs. For the case of Zn-doped InP, all depressions were surrounded by noncentrosymmetric maxima. We cannot give a satisfactory explanation for these maxima at present.

Upon moving the tip Fermi level to the bottom of the conduction band, we observed that the depressions turned into elevations with a triangular shape for the Zn- and Cd-doped GaAs, and the Zn-doped InP. The chemical nature of the dopants (Zn or Cd) did not influence this triangular shape, and the depth of the dopants did not have any

influence on the shape either. The orientation of these triangular features was the same for all observed doping atoms and was geometrically determined with respect to the host lattice. The location of a triangular feature with respect to a doping atom was also determined. The features were only visible when tunneling to the impurity band suggesting that the features are a direct image of the acceptor state although their precise origin is still unclear.

ACKNOWLEDGMENTS

We would like to thank J. G. H. Hermsen and J. W. Geritsen for their technical assistance. Part of this work was supported by the Stichting Fundamenteel Onderzoek der Materie (FOM), which is financially supported by the Nederlandse Organisatie voor Wetenschappelijk Onderzoek (NWO).

-
- ¹C. Domke, M. Heinrich, Ph. Ebert, and K. Urban, *J. Vac. Sci. Technol. B* **16**, 2825 (1998).
- ²M.B. Johnson, O. Albrechtsen, R.M. Feenstra, and H.W.M. Salemink, *Appl. Phys. Lett.* **63**, 2923 (1993); **64**, 1454(E) (1994).
- ³J.F. Zheng, X. Liu, N. Newman, E.R. Weber, D.F. Ogletree, and M. Salmeron, *Phys. Rev. Lett.* **72**, 1490 (1994).
- ⁴Ph. Ebert, M. Heinrich, M. Simon, C. Domke, K. Urban, C.K. Shih, M.B. Webb, and M.G. Lagally, *Phys. Rev. B* **53**, 4580 (1996).
- ⁵For our InP(110) surfaces, we estimated the maximum depth at which a doping atom is positioned and can still be observed to be 3.3 nm. This corresponds to 15 subsurface layers. For our GaAs(110) surfaces, we obtained similar results (Ref. 7).
- ⁶M.C.M.M. van der Wielen, A.J.A. van Roij, and H. van Kempen, *Phys. Rev. Lett.* **76**, 1075 (1996).
- ⁷M.C.M.M. van der Wielen, Ph.D. thesis, University of Nijmegen, 1998.
- ⁸J.F. Zheng, M. Salmeron, and E.R. Weber, *Appl. Phys. Lett.* **64**, 1836 (1994); **65**, 790(E) (1994).
- ⁹R.M. Feenstra, J.M. Woodall, and G.D. Pettit, *Phys. Rev. Lett.* **71**, 1176 (1993).
- ¹⁰R.B. Capaz, K. Cho, and J.D. Joannopoulos, *Phys. Rev. Lett.* **75**, 1811 (1995).
- ¹¹B. Grandidier, Huajie Chen, R.M. Feenstra, D.T. McInturff, P.W. Juodawlkis, and S.E. Ralph, *Appl. Phys. Lett.* **74**, 1439 (1999).
- ¹²J.W.G. Wildöer, A.J.A. van Roij, H. van Kempen, and C.J.P.M. Harmans, *Rev. Sci. Instrum.* **65**, 2849 (1994).
- ¹³The doping concentrations were copied from the specification lists enclosed with the commercially bought wafers. The doping concentration of the Zn-doped InP was verified by electrical conductivity measurements performed by P. M. Koenraad *et al.* from the Eindhoven University of Technology.
- ¹⁴This method has been described before by Johnson *et al.* (Ref. 2) and Ebert *et al.* (Ref. 4).